Advances in Mechanical and Materials Engineering

Volume 41, 2024, Pages 221-231
https://doi.org/10.7862/rm.2024.19

THE FACULTY OF MECHANICAL ENGINEERING AND AERONAUTICS
RZESZOW UNIVERSITY OF TECHNOLOGY

Original Research

Effect of Single-Point Incremental Forming Process Parameters on Roughness of the Outer Surface of Conical Drawpieces from CP Titanium Sheets

Marcin Szpunar [1,*], Robert Ostrowski [2], Andrzej Dzierwa [3]

[1] MTU Aero Engines Polska, Tajęcina 108, 36-002 Jasionka, Poland
[2] Department of Materials Forming and Processing, Faculty of Mechanical Engineering and Aeronautics, Rzeszów University of Technology, al. Powstancow Warszawy 8, 35-959 Rzeszow, Poland; rostrows@prz.edu.pl
[3] Department of Manufacturing and Production Engineering, Faculty of Mechanical Engineering and Aeronautics, Rzeszów University of Technology, al. Powstancow Warszawy 8, 35-959 Rzeszow, Poland; adzierwa@prz.edu.pl

* Correspondence: marcin.szpunar@outlook.com

Received: 7 November 2024 / Accepted: 18 December 2024 / Published online: 30 December 2024

Abstract

With the widespread use of numerically controlled machine tools, single-point incremental forming (SPIF) process has enjoyed growing interest in the industry. This article presents the results of research on the influence of forming process parameters (step size, tool rotational speed, feed rate and forming strategy) on the roughness of the outer surface of conical drawpieces with a slope angle of 45° from commercially pure titanium sheets. The following variable process parameters were used: tool rotational speed varied from –600 to 600 rpm, feed rate varied from 500 to 2000 mm/min and step size varied from 0.1 to 0.5 mm. The SAE 75W85 synthetic gear oil was used as lubricant. Two basic roughness parameters were analyzed: the mean roughness Sa and the maximum height Sz. The influence of SPIF parameters on surface roughness was analysed using multi-layer artificial neural networks. It was found that reducing the feed rate with the climb strategy causes a decrease in the average roughness Sa. The opposite relationship was observed when forming according to the conventional strategy. At low tool feed rate (500 mm/min), reducing the step size caused an increase in the Sz parameter. At high tool feed rate (2000 mm/min), the effect of the step size is negligible.

Keywords: artificial neural networks, incremental sheet forming, sheet metal forming, SPIF, surface roughness

1. Introduction

Single-point incremental forming (SPIF) is a method of machining components made of sheet metal. The SPIF process involves the gradual forming of sheet metal using a pin tool moving along a programmed trajectory adapted to the shape of the drawpiece. The incremental forming processes are highly flexible, allowing different parts to be manufactured using the same tooling system, leading to significant material and energy savings. Additionally, the process offers lower costs and shorter lead times compared to conventional forming methods (Petek et al., 2007). Despite the many advantages of incremental forming, SPIFed components are sensitive to reduced surface roughness, geometric deviations and high springback (Najm & Paniti, 2023; Rosca et al., 2019). The deterioration of surface roughness is the result of frictional interaction between the tool surface and the sheet metal surface (Najm & Paniti, 2021a; Paniti et al., 2020). Additionally, on the opposite (outer) side of the drawpiece wall, an intensive change in surface topography occurs due to deformations of the sheet material. The effect is commonly called ‘orange peel patterns’ (Liao et al., 2020). The deterioration of the internal surface of the drawpieces is related to the small area of real contact of the forming tool with the sheet metal and severe friction conditions. Too much friction can lead to premature sheet metal fracture.

A common way to reduce friction is to use lubricants with properties adapted to the processing parameters (Milutinović, 2021).

The SPIF technique can be used to form practically all types of metallic materials that are formed using conventional sheet metal forming methods. Titanium sheets, due to their high mechanical strength and low weight, are used in the aviation industry and in luxury cars. The very good biocompatibility of titanium and its alloys makes these materials widely used as medical prostheses (Oleksik et al., 2010). Titanium exhibits good corrosion resistance due to its natural passivation in an atmosphere containing oxygen. The passive TiO_2 layer makes these materials resistant to seawater, weather conditions and chemicals. In the literature, SPIF applications can be found for forming hip prostheses (Sbayti et al., 2016), denture plates (Sbayti et al., 2018) and cranial implants (Cotigă et al., 2014).

The significant factors influencing the obtained surface roughness of the drawpieces include the step size (the smaller the step size, the lower the surface roughness), the tool diameter (the smaller the diameter, the lower the surface roughness) and the forming angle of the drawpiece (the larger the angle, the lower the surface roughness). The tool rotational speed value also has a significant effect on the resulted surface quality, but this is a more complex effect, which also depends on other process parameters. In terms of tool rotation, forming with a rotary tool is more advantageous than with stationary (non-rotating) tool (Hagan & Jeswiet, 2004). Friction in SPIF methods is difficult to analyse qualitatively and quantitatively due to the occurrence of severe mechanical interactions of the cooperating surfaces of tool and blank. This intensifies the adhesive wear phenomena, directly affecting the formability and surface quality of the components (Oleksik et al., 2008). Providing appropriate contact conditions is particularly important when forming titanium, aluminium and their alloy sheets (Najm & Paniti, 2020; 2021a). The improvement of sheet formability can be achieved by implementing the SPIF process at elevated temperature (Popp et al., 2024). Mainly, heating of the workpiece using a stream of hot air, resistance heating, a laser beam or ultrasound is used. Recent research also focuses on improving the geometric quality of parts manufactured by the SPIF techniques by optimising the forming process conditions, lubrication (Şen et al., 2022), numerical techniques such as the finite element method (Pepelnjak et al., 2022) and metamodeling (Sbayti et al., 2022).

The proper selection of SPIF parameters is a key issue for obtaining the required quality of drawpieces. There are many sources in the literature devoted to the influence of SPIF process parameters on the value of forming force, coefficient of friction, springback of the material, temperature in the contact zone and the maximum forming angle (Blaga et al., 2012). Due to many factors that simultaneously synergistically affect the course of SPIF and effects of the forming process, researchers often focus on the optimisation of a selected parameter, such as the surface roughness of the inner or outer surface of the drawpiece, the tool path and the geometric accuracy of the component shape (Najm & Paniti, 2021b). Methods for optimising forming parameters using machine learning and artificial neural networks are also used (Racz et al., 2019). Najm and Paniti (2023) used multilayer neural network for studying the effect of SPIF parameters on prediction of the wall diameter and pillow effect. The best performance of ANN was achieved by way of the Levenberg–Marquardt training algorithm. In another paper by Najm and Paniti (2021a) the ANNs were used to predict surface roughness parameters Sa and Rz, measured on the inner surface of the SPIFed frustum cones. The results showed that ANN gives a better result than support vector regression. Racz et al. (2019) used an adaptive network-based fuzzy inference system to extract the value of thrust force, which appears during incremental forming of DC04 steel drawpieces. The proposed method offering effective method for estimating the forces in SPIF. Oraon and Sharma (2021) applied ANN for predicting the average surface roughness Ra of SPIFed drawpieces from celamine brass Cu67Zn33. The overall efficiency of proposed ANN model was 94.7%. Choundary et al. (2025) predicted formability of material in SPIF of EN AW-7075-T6 aluminium alloy varying wall angle conical frustums by using single-output and double-output ANNs. It was concluded that the developed model allows to reduce the cost and time to select accurate SPIF parameters without performing expensive experiments. The application of artificial intelligence techniques in incremental sheet forming methods was presented by Nagargoje et al. (2023).

Most of the experimental studies of SPIF focus on the analysis of changes in the topography of the inner surface of the drawpieces. This surface is important from the technological point of view. However, the outer surface is often painted and further processed, which also requires meeting certain quality requirements. This article focuses on the analysis of the influence of SPIF process parameters (step size, tool rotational speed, feed rate and forming strategy) on the quality of the outer surface of conical drawpieces from commercially pure (CP) titanium sheets. The effect of tool rotation direction in relation to feed direction on surface roughness has not been the subject of many studies. This aspect

was also taken into account in our research. Due to the difficult to interpret relationship between input parameters and surface roughness, multilayer artificial neural networks were used.

2. Materials and methods

2.1. Workpiece

Incremental forming tests were conducted using 0.4-mm-thick CP titanium sheets grade 2 in annealed state. Chemical composition of the CP titanium sheet according to the requirements of the ASTM B348 (American Society for Testing and Materials, 2019) standard are presented in Table 1. The mechanical properties of the sheets were determined using a static uniaxial tensile test. The test specimens were cut along the rolling direction (RD). Three specimens were tested and on this basis the average values of selected mechanical parameters were determined. The average values of the basic mechanical parameters are presented in Table 2. The surface roughness parameters of the blanks were measured using a Bruker Contour GT 3D optical profilometer, in accordance with the ISO 25178 standard (International Organization for Standardization, 2019). The values of the basic surface roughness parameters were: Sa = 0.458 µm, Sz = 4.63 µm, Sp = 2.17 µm and Sv = 2.46 µm.

Table 1. Chemical composition (max., wt.%) of CP titanium sheet

Fe	C	O	N	H	Ti
0.3	0.1	0.25	0.03	0.015	balance

Table 2. Results of uniaxial tensile tests for CP titanium sheets

Yiels stress $R_{p0.2}$ MPa	Ultimate tensile strengths R_m, MPa	Elongation at fracture A, %
463.0	616.2	21.6

2.2. Experimental procedure

Experiment was carried out on 3-axis milling CNC machine Makino PS95. Inside machine working space, specially created device (Fig. 1) for incremental sheet forming was mounted. The device allows to fix up to Ø100 mm sheet blanks and such a titanium sheets were used in experiment. Ø8 mm hemispherical tool, made of sintered tungsten carbide was applied to punch. Conical drawpiece with a constant wall angle of 45° (Fig. 2) was selected as a specimen. Such a geometry allowed to achieve specimen height up to 28.3 mm while starting from cone diameter Ø60 mm. Siemens NX CAM module was used to generate spiral tool paths with constant step size. The tool path was generated based on the desired drawpiece geometry (Fig. 2). The conventional SPIF and climb SPIF (Fig. 3) were considered. To improve friction conditions between tool and sheet, SAE 75W85 synthetic gear oil was used. The SAE 75W-85 gear oil used in the tests provided adequate lubrication at the tool-sheet interface. This lubricant was selected based on preliminary tests and work by Krasowski (2021) on incremental forming of aluminium alloy sheets that are subject to galling.

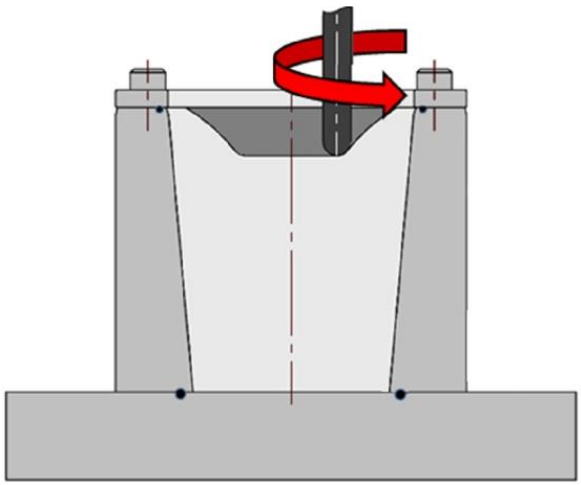

Fig. 1. Test stand configured for the experiment.

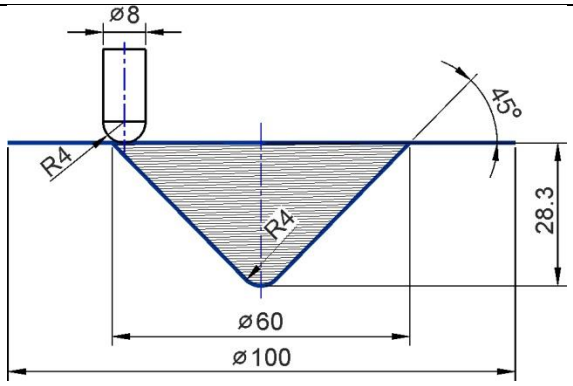

Fig. 2. Geometry and dimensions (in mm) of the tool and the drawpiece.

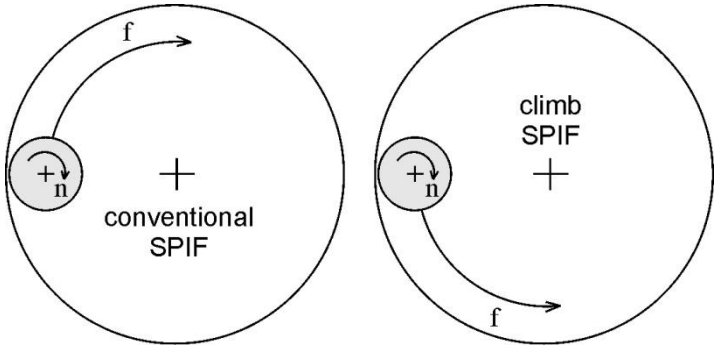

Fig. 3. The concept of conventional and climb SPIF.

Central composite design (CCD) was established to evaluate effect of forming parameters such as tool rotational speed, feed rate and step size on inner and outer drawpiece surface quality. The following variable process parameters were used: tool rotational speed varied from –600 to 600 rpm, feed rate varied from 500 to 2000 mm/min and step size varied from 0,1 to 0.5 mm. Placing some experimental runs outside the minimum and maximum factor ranges in CCD is a conscious strategy to obtain more accurate and useful results, which translates into a better understanding of the process being studied. Rotational speed values below zero means that the direction of the rotation has been switched to opposite (from left to right). Such a combination of input parameters with CCD plan results in 20 runs, where only drawpieces formed completely (without crack) were taken into account. Details of experiments are presented in paper (Szpunar et al., 2021). Only for some settings of SPIF parameters it was possible to form the drawpieces with the desired height h = 28.3 mm. This article focuses on modeling the surface roughness changes for successfully formed drawpieces with parameters shown in Table 3.

Surface topographies were measured in an area of 3.0 × 2.5 mm at a location at half the height of the drawpieces (Fig. 4) using a Talysurf CCI Lite profilometer. The average roughness Sa and the maximum height of profile Sz were selected as roughness parameters for the analysis of topography changes of the outer surface of the drawpieces. Due to the cyclic character of topography changes resulting from the movement of the tool along the spiral trajectory, these parameters are most often used and recommended for the analysis of topography of SPIFed components (Kurra et al., 2015).

Table 3. Experiment design according to central composite design.

Test no.	Step size a_p, mm	Feed rate f, mm/min	Tool rotational speed n, rpm	Drawpiece height h, mm
1	0.3	1250	–200	28.3
2	0.1	2000	–600	28.3
3	0.3	1250	–790	28.3
4	0.5	500	600	28.3
5	0.3	1250	–400	28.3
6	0.1	500	600	28.3
7	0.1	500	–600	28.3
8	0.3	1250	790	28.3
9	0.5	2000	–600	28.3
10	0.5	2000	600	28.3
11	0.5	500	–600	28.3
12	0.3	1250	400	28.3

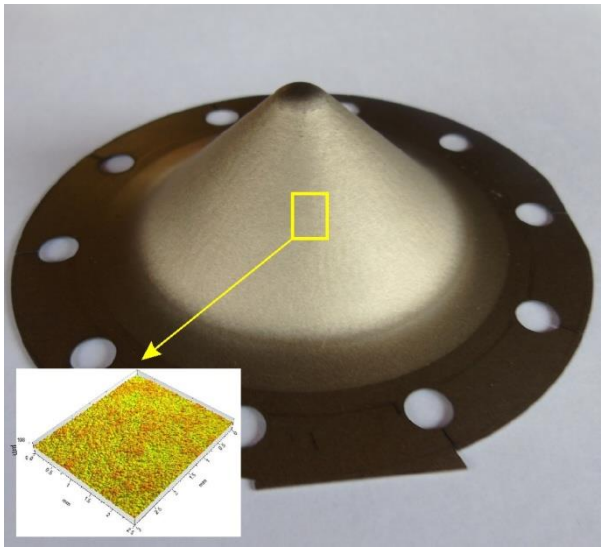

Fig. 4. Place of measurement of the surface topography of the drawpieces.

2.3. Artificial neural networks

To analyse the influence of SPIF parameters on the roughness of the outer surface of the drawpieces, multilayer artificial neural networks (ANNs) were used, which are a module in the Statistica program. The input parameters were step size, tool rotational speed, feed rate and forming strategy. In the case of conventional strategy, the velocity value was negative (Szpunar et al., 2021). Neural networks with one output neuron were used. According to Garret et al. (1997), such an architecture is sufficient to model any complex task. Separate networks were built taking into account the average roughness Sa and maximum height of profile Sz at the output (Fig. 5).

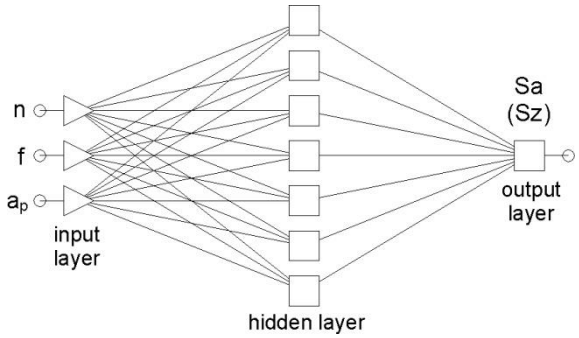

Fig. 5. Architecture of ANN used.

After entering the input data into Statistica and normalizing them to the interval <0, 1>, the program automatically performs the analysis for many ANN architectures with different numbers of neurons in the output layer and determines the ANN with the best quality. A validation set was separated from the training set and 20% of the data sets were randomly assigned to this set. The back propagation algorithm with momentum 0.3 and learning rate 0.1. was used to train the networks. This is the most commonly used and considered the most effective algorithm for training multilayer ANNs. The coefficient of determination R^2 between the experimental and predicted data was adopted as the network quality indicator (Najm & Paniti, 2021b):

$$R^2 = \frac{\sum_{i=1}^{n}(y_i^a - \bar{y})^2 - \sum_{i=1}^{n}\left(y_i^a - y_i^p\right)^2}{\sum_{i=1}^{n}(y_i^a - \bar{y})^2} \tag{1}$$

where n is number of measurement, y_i^p is the prediction value of specific surface roughness parameter, y_i^a is the actual value of specific surface roughness parameter and $\bar{y}$ is the average value of specific surface roughness parameter.

3. Results and discussion

The surface of the components formed with different machining parameters (Table 2) was characterised by a rough structure resulting from the formation of the 'orange peel' effect. This mechanism is created by the change in the orientation of the material grains caused by high subsurface stresses. The outer surface of the drawpiece, during the interaction of the tool with its inner surface, is subjected to local bending and tensile loads (Fang et al., 2014). The occurrence of such loads favours the occurrence of sheet metal surface defects in the form of voids and microcracks. The orange peel effect, presented in the photographs of the surfaces of selected incrementally formed drawpieces (Fig. 6), was first described by Hosford and Caddell (1983). During SPIF processing, the grains of the internal structure of the sheet material tend to thin out or change orientation. The outer surface of the drawpieces takes on a rough appearance due to the different orientations of the neighbouring grains on the surface (Hamilton & Jeswiet, 2010). Due to the character of the orange peel, the outer surfaces of the drawpieces can be divided into three groups: surfaces with a uniform surface of low roughness (Fig. 6a), surfaces with horizontal marks corresponding to the tool engagement on the inner surface of the drawpiece (Fig. 6b), and surfaces with high roughness with uneven valleys (Fig. 6c).

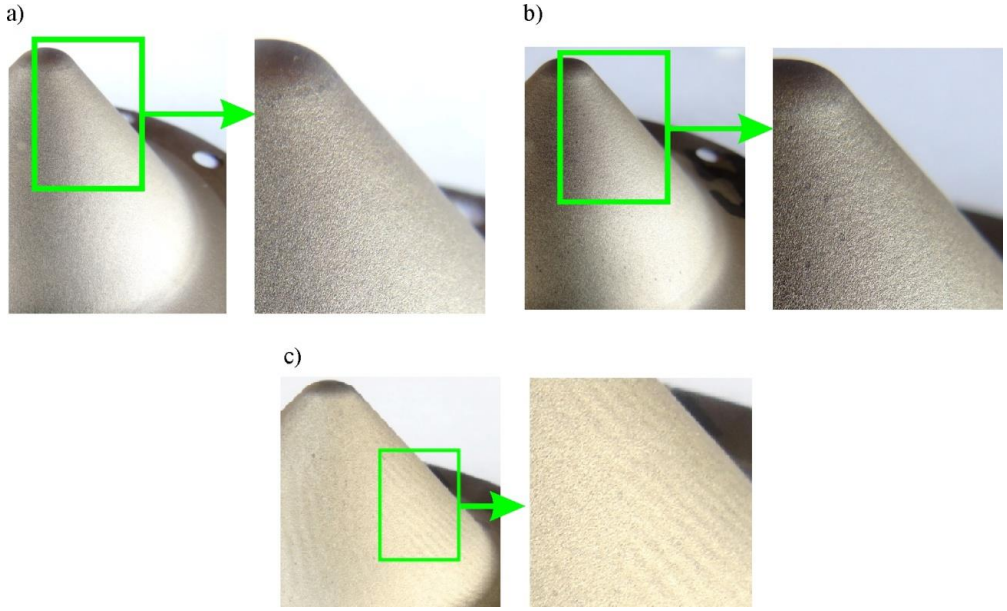

Fig. 6. Outer surface of the drawpieces formed at: a) n = 400 rpm, f = 1250 mm/min, a_p = 0.3 mm, climb strategy; b) n = 600 rpm, f = 2000 mm/min, a_p = 0.5 mm, conventional strategy; c) n = 600 rpm, f = 500 mm/min, a_p = 0.1 mm, conventional strategy.

Average roughness values and maximum height of profile are shown in Table 4. The average roughness values varied between 2.77 and 3.98 µm. The maximum height of profile varied in a much larger range between 74 and 239 µm. It should be mentioned that average roughness Sa and maximum height of profile Sz of as-received sheet metal were 0.458 µm and 4.63 µm, respectively. The outer surface topographies of the selected drawpieces are shown in Fig. 7. The outer surface of the drawpieces consists of evenly distributed dimples (Fig. 8). At high magnification (Fig. 8d) one can see dimples of various sizes, the character of which is similar to the surface of a ductile fracture.

Table 4. Selected surface roughness parameters measured on the outer surface of the cones.

Test no.	Sa, µm	Sz, µm
1	2.77	74.3
2	3.98	136
3	3.4	108
4	3.7	168
5	3.21	239
6	3.42	100
7	3.45	142
8	3.55	195
9	3.38	149
10	2.83	74
11	3.38	103
12	2.95	74.8

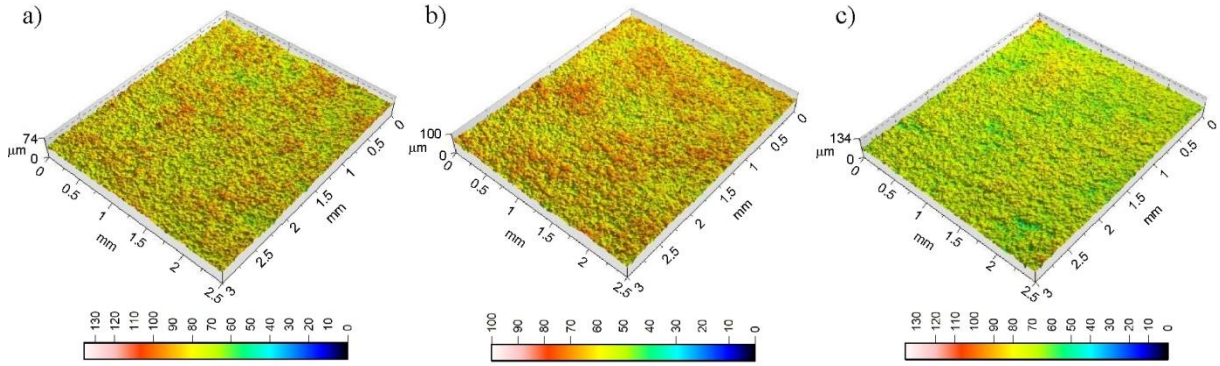

Fig. 7. Topography of the outside surface of the drawpieces formed at a) a_p = 0.5 mm, f = 1250 mm/min, n = –200 rpm; b) a_p = 0.1 mm, f = 500 mm/min, n = 600 rpm and c) a_p = 0.1 mm, f = 2000 mm/min, n = –600 rpm.

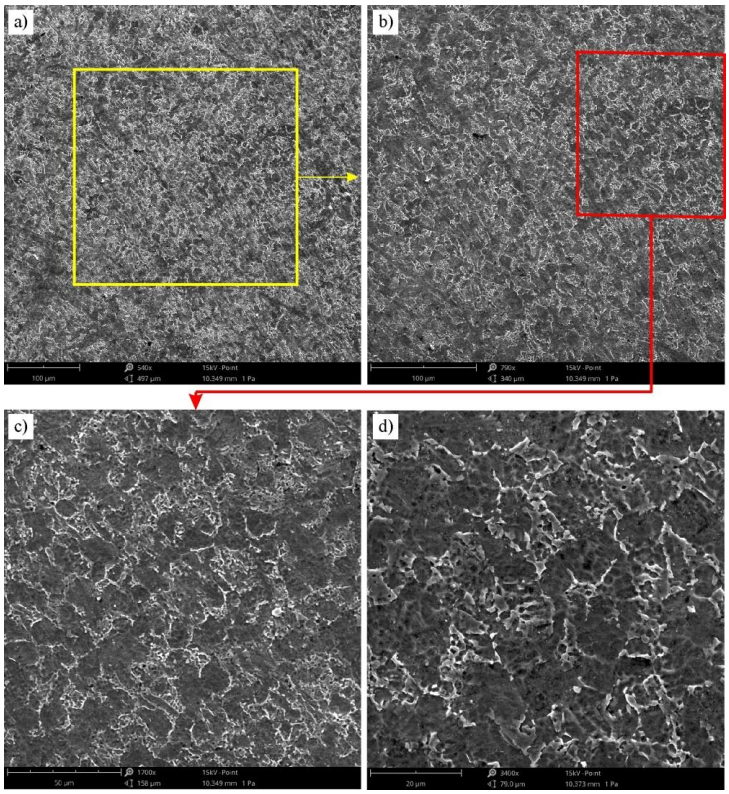

Fig. 8. SEM micrographs of the outer surface of the drawpiece formed with n = 790 rpm, f = 1250 mm/min ap = 0.3 mm, conventional strategy, at magnifications: a) 540×, b) 790×, c) 1700× and d) 3400×.

After data analysis, the Statistica program proposed the best network architecture, separately for the Sa parameter and separately for the Sz parameter. In both cases, it was a network with 7 neurons in the hidden layer: ANN 3:3-7-1:1. The regression statistics of the obtained networks are presented in Table 5. The coefficients of determination R^2 for both networks exceed 0.92 (0.98 for analysed Sa parameter), so it can be assumed that the neural networks satisfactorily reproduce the experimental data. It should be noted that the amount of training data was not large, and yet the ANNs adapted to the training data in an acceptable way.

Table 5. Regression statistics of ANNs.

Output variable	Sa	Sz
data mean	3.307	131.41
standard deviation of data	0.3806442	55.98477
error mean	0.0001329	0.001395
standard deviation of errors	0.07404	28.94689
absolute terror mean	0.03912	20.51552
standard deviation ratio	0.1945242	0.5170494
Coefficient oif determination R^2	0.9809132	0.922311

Analyzing the response surfaces for average roughness as output variable (Fig. 9), it can be seen that the average roughness of the outer surface of drawpieces is sensitive to the change of tool rotational speed (Figs. 9a and 9b) in relation to the direction of feed rate (forming strategy). In conventional strategy, the values of the Sa parameter are definitely higher than during forming with the climb strategy. Increasing the feed rate with the climb strategy causes an increase in the Sa parameter (Fig. 9a). The opposite relationship occurs when forming according to the conventional strategy (Fig. 9a). It can be stated that the step size, when we consider this parameter together with the tool rotational speed (Fig. 9b), has a small effect on the average roughness. The effect of the step size in interaction with the feed rate is more significant (Fig. 9c). At low feed rate (500 mm/min), increasing the step size causes an increase in the Sa parameter. At high feed rate (2000 mm/min), increasing the step size reduces the average roughness. The rotational speed determines the frictional interaction of the tools with the sheet metal surface. A small feed rate causes faster local heating of the surface asperities, which on the one hand facilitates the forming of the sheet metal, but at the same time at an elevated temperature the tool has a more intensive impact on the deterioration of the surface quality (Fig. 9c).

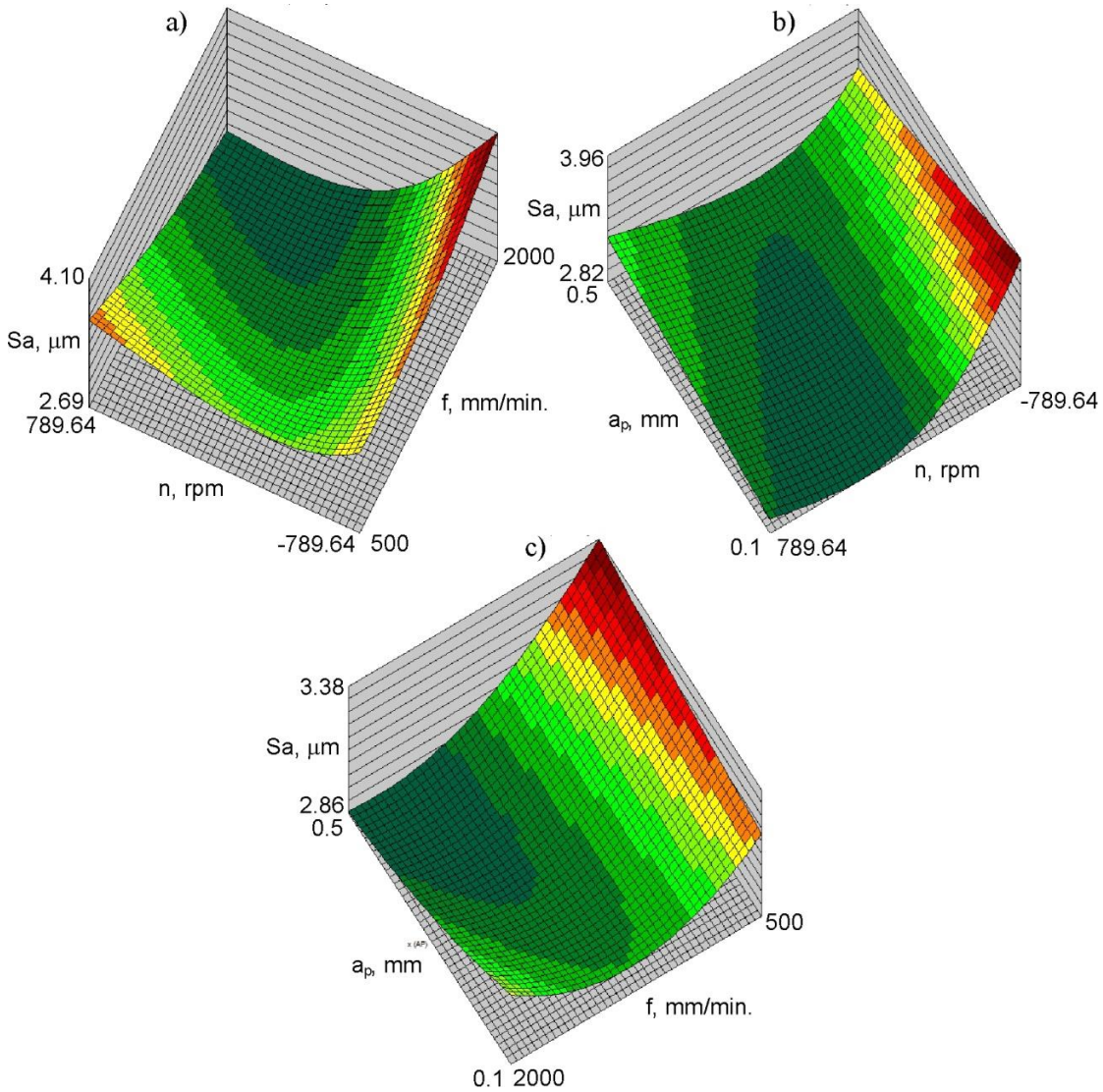

Fig. 9. Response surfaces of ANN showing the effect of a) tool rotational speed and feed rate, b) step size and tool rotational speed, and (c) step size and feed rate on the value of Sa parameter.

Figure 10 shows the response surfaces for maximum height of profile Sz. At a small tool feed rate (500 rpm), increasing the step size causes a decrease in the Sz parameter. At a large tool feed rate (2000 rpm), the effect of the step size is negligible. The effect of feed rate in combination with step size (Fig. 10c) is rather clear, increasing the feed rate increases the maximum height of profile of outer surface. The effect of tool rotational speed and step size (Fig. 10a), and feed rate and tool rotational speed (Fig. 10b) is more complex. Regardless of the rotational speed, decreasing the step size causes an increase in the Sz parameter (Fig. 10a).

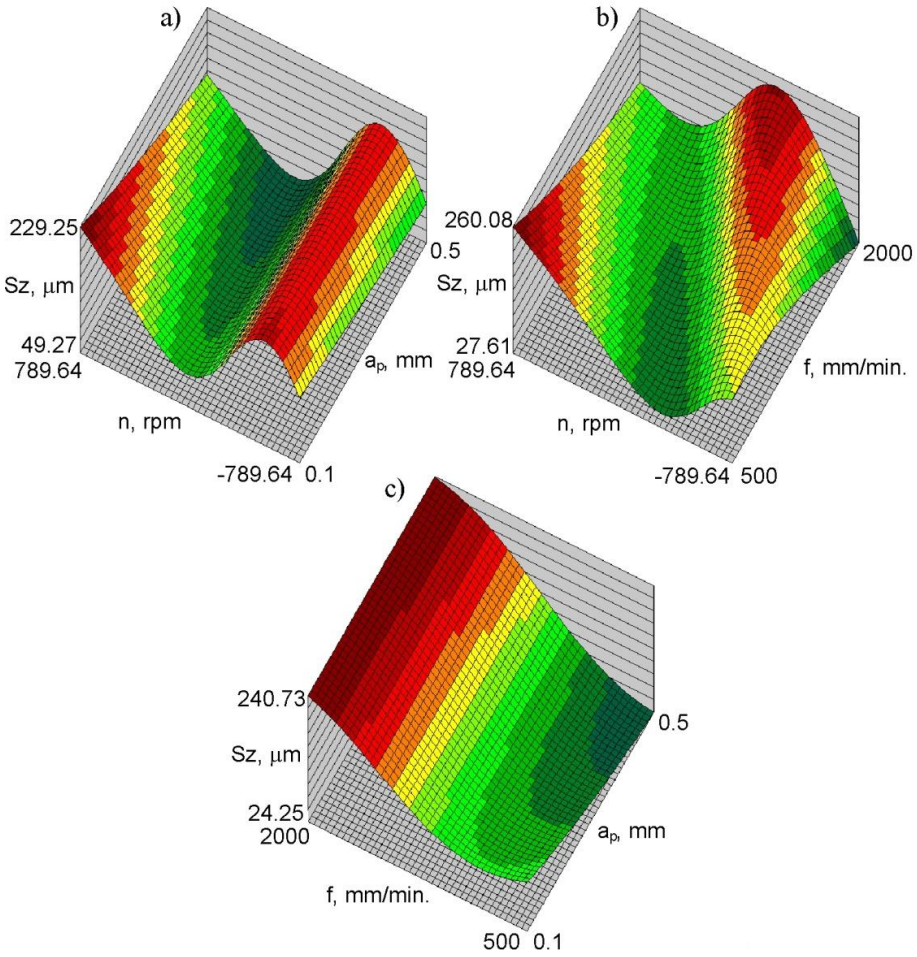

Fig. 10. Response surfaces of ANN showing the effect of a) tool rotational speed and step size, b) feed rate and tool rotational speed, and (c) step size and feed rate on the value of Sz parameter.

4. Conclusions

The article presents the results of experimental studies of changes in basic surface roughness parameters during the forming of conical drawpieces from commercially pure thin titanium sheets and their analysis using multilayer artificial neural network models. The conducted analyses allow for the following main conclusions to be drawn:

- The change in the topography of the outer surface of the drawpieces, depending on the forming parameters, can have a different character: uniform topography with low roughness, topography with horizontal marks corresponding to the tool engagement on the inner surface of the drawpiece and topography with high roughness with uneven valleys.
- Orange peel effect leads to plastic deformation of surface asperities, causing the formation of a grid with small dimples on the sheet metal surface, which roughly correspond to the view of ductile fracture.
- Based on the response surfaces of ANN, it can be stated that in the conventional strategy the average roughness Sa values are higher than during machining with the climb strategy. Reducing the feed rate with the climb strategy causes a decrease in the Sa parameter. The opposite relationship occurs when forming according to the conventional strategy.
- At a small tool feed rate (500 mm/min), reducing the step size causes an increase in the Sz parameter. At a large tool feed rate (2000 mm/min), the effect of the step size on the Sz parameter is negligible.

In future studies, it is planned to analyse the type of lubricant on the surface roughness of the inner and outer surfaces of the drawpieces. In addition, a problem that does not find wide research interest in the literature is the effect of the tool surface roughness on the resulting surface roughness of the drawpiece formed by the SPIF technique. Increasing the amount of training data will affect the better quality of the neural network models.

References

American Society for Testing and Materials. (2019). *Standard specification for titanium and titanium alloy bars and billets* (ASTM Standard No. B348-13). https://www.astm.org/standards/b348

Blaga, A., Bologa, O., Oleksik, V., & Pirvu, B. (2012). Experimental researches regarding the influence of geometric parameters on the principal strains and thickness reduction in single point incremental forming. *UPB Scientific Bulletin, Series D: Mechanical Engineering*, *74*(2), 111-120.

Choudhary, S., Chounchary, N., Kumari, S., Kumari, A., & Mulay, A. (2025). Application of artificial neural network in predicting the performance of SPIF for aerospace grade AA7075-T6. *Journal of Alloys and Compounds*, *1010*, Article 177146. https://doi.org/10.1016/j.jallcom.2024.177146

Cotigă, C., Bologa, O., Racz, S. G., & Breaz, R. E. (2014). Researches regarding the usage of titanium alloys in cranial implants. *Applied Mechanics and Materials*, *657*, 173–177. https://doi.org/10.4028/www.scientific.net/AMM.657.173

Fang, Y., Lu, B., Chen, J., Xu, D. K., & Ou, H. (2014). Analytical and experimental investigations on deformation mechanism and fracture behavior in single point incremental forming. *Journal of Materials Processing Technology*, *214*(8), 1503–1515. https://doi.org/10.1016/j.jmatprotec.2014.02.019

Garret, J. H., Gunarathan, D. J, & Ivezic, N. (1997). Introduction. In N. Kartam, I. Flood, J. H. Garrett (Eds.), *Artificial neural networks for civil engineers: Fundamentals and applications* (pp. 1-18). American Society of Civil Engineers.

Hagan, E., & Jeswiet, J. (2004). Analysis of surface roughness for parts formed by computer numerical controlled incremental forming. *Proceedings of the Institution of Mechanical Engineers, Part B: Journal of Engineering Manufacture*, *218*(10), 1307-1312. https://doi.org/10.1243/0954405042323559

Hamilton, K., & Jeswiet, J. (2010). Single point incremental forming at high feed rates and rotational speeds: Surface and structural consequences. *CIRP Annals*, *59*(1), 311–314. https://doi.org/10.1016/j.cirp.2010.03.016

Hosford, W., & Caddell, R. (1983). *Metal forming*. Prentice Hall.

International Organization for Standardization. (2019). *Geometrical product specifications (GPS) — Surface texture: Areal* (ISO Standard No. ISO 25178-600:2019). https://www.iso.org/standard/67651.html

Krasowski, B. (2021). *Analiza procesu kształtowania przyrostowego usztywnień w cienkościennych konstrukcjach nośnych wykonanych ze stopów aluminium EN AW-2024-T3 oraz EN AW-7075-T6* [Doctoral dissertation, Rzeszów University of Technology].

Kurra, S., Rahman, N. H., Regalla, S. P., & Gupta, A. K. (2015). Modeling and optimization of surface roughness in single point incremental forming process. *Journal of Materials Research and Technology*, *4*(3), 304–313. https://doi.org/10.1016/j.jmrt.2015.01.003

Liao, J., Liu, J., Zhang, L., & Xue, X. (2020). Influence of heating mode on orange peel patterns in warm incremental forming of magnesium alloy. *Procedia Manufacturing*, *50*, 5-10. https://doi.org/10.1016/j.promfg.2020.08.002

Milutinović, M., Lendjel, R., Baloš, S., Zlatanović, D. L., Sevšek, L, Pepelnjak, T. (2021). Characterisation of geometrical and physical properties of a stainless steel denture framework manufactured by single-point incremental forming. *Journal of Materials Research and Technology*, *10*, 605-623. https://doi.org/10.1016/j.jmrt.2020.12.014

Nagargoje, A., Kankar, P. K., Jain, P. K., & Tandon, P. (2023). Application of artificial intelligence techniques in incremental forming: A state-of-the-art review. *Journal of Intelligent Manufacturing*, *34*, 985–1002. https://doi.org/10.1007/s10845-021-01868-y

Najm, S. M., & Paniti, I. (2020). Study on effecting parameters of flat and hemispherical end tools in SPIF of aluminium foils. *Technical Gazette*, *27*(6), 1844-1849. https://doi.org/10.17559/TV-20190513181910

Najm, S. M., & Paniti, I. (2021a). Predict the effects of forming tool characteristics on surface roughness of aluminum foil components formed by SPIF using ANN and SVR. *International Journal of Precision Engineering and Manufacturing*, *22*(1), 13-26. https://doi.org/10.1007/s12541-020-00434-5

Najm, S. M., & Paniti, I. (2021b). Artificial neural network for modeling and investigating the effects of forming tool characteristics on the accuracy and formability of thin aluminum alloy blanks when using SPIF. *International Journal of Advanced Manufacturing Technology*, *114*, 2591–2615. https://doi.org/10.1007/s00170-021-06712-4

Najm, S. M., & Paniti, I . (2023). Investigation and machine learning-based prediction of parametric effects of single point incremental forming on pillow effect and wall profile of AlMn1Mg1 aluminum alloy sheets. *Journal of Intelligent Manufacturing*, *34*(1), 331-367. https://doi.org/10.1007/s10845-022-02026-8

Oleksik, V., Bologa O., Breaz, R., & Racz, G. (2008). Comparison between the numerical simulations of incremental sheet forming and conventional stretch forming process. *International Journal of Material Forming*, *1*, 1187-1190. https://doi.org/10.1007/s12289-008-0153-6

Oleksik, V., Pascu, A., Deac, C., Fleacă, R., Bologa, O., & Racz, G. (2010). Experimental study on the surface quality of the medical implants obtained by single point incremental forming. *International Journal of Material Forming*, *3*, 935-938. https://doi.org/10.1007/s12289-010-0922-x

Oraon, M., & Sharma, V. (2021) Application of artificial neural network: A case of single point incremental forming (SPIF) of Cu67Zn33 alloy. *Management and Production Engineering Review*, *12*(1), 17-23. https://doi.org/10.24425/mper.2021.136868

Paniti, I., Viharos, Z. J., Harangozó, D., & Najm, S. M. (2020). Experimental and numerical investigation of single point incremental forming of aluminium alloy foils. *Acta Imeko*, *9*(1), 25-31. https://doi.org/10.21014/acta_imeko.v9i1.750

Pepelnjak, T., Sevšek, L., Lužanin, O., & Milutinović M. (2022). Finite element simplifications and simulation reliability in single point incremental forming. *Materials*, *15*(10), Article 3707. https://doi.org/10.3390/ma15103707

Petek, A., Gantar, G.; Pepelnjak, T., & Kuzman K. (2007). Economical and ecological aspects of single point incremental forming versus deep drawing technology. *Key Engineering Materials*, *344*, 931-938. https://doi.org/10.4028/www.scientific.net/KEM.344.931

Popp, G. P., Racz, S. G., Breaz, R. E., Oleksik, V. Ș., Popp, M. O., Morar, D. E., Chicea, A. L., Popp, I. O. (2024). State of the art in incremental forming: process variants, tooling, industrial applications for complex part manufacturing and sustainability of the process. *Materials*, *17*(23), Article 5811. https://doi.org/10.3390/ma17235811

Racz, S. G., Breaz, R. E., Bologa, O., Tera, M., & Oleksik V. S. (2019). Using an adaptive network-based fuzzy inference system to estimate the vertical force in single point incremental forming. International *Journal of Computers Communications & Control*, *14*(1), 63-77.

Rosca, N., Oleksik, V., Pascu, A., Oleksik, M., & Avrigean E. (2019). Optical study for springback prediction, thickness reduction and forces variations on single point incremental forming. *Materials Today: Proceedings*, *12*, 213-218. https://doi.org/10.1016/j.matpr.2019.03.116

Şen, N., Şirin, Ş., Kıvak, T., Civek, T., & Seçgin, Ö. (2022). A new lubrication approach in the SPIF process: Evaluation of the applicability and tribological performance of MQL. *Tribology International*, *171*, Article 107546. https://doi.org/10.1016/j.triboint.2022.107546

Sbayti, M., Bahloul, R., & Belhadjsalah, H. (2018). Numerical modeling of hot incremental forming process for biomedical application. In M. Haddar, F. Chaari, A. Benamara, M. Chouchane, C. Karra, N. Aifaoui (Eds.), *Design and modeling of mechanical systems—III* (pp. 881-891). Springer International Publishing. https://doi.org/10.1007/978-3-319-66697-6_86

Sbayti, M., Ghiotti, A., Bahloul, R., Belhadjsalah, H., & Bruschi, S. (2016). Finite element analysis of hot single point incremental forming of hip prostheses. *MATEC Web of Conferences*, *80*, Article 14006. https://doi.org/10.1051/matecconf/20168014006

Sbayti, M., Ghiotti, A., Bahloul, R., BelhadjSalah, H., & Bruschi, S. (2022). effective strategies of metamodeling and optimization of hot incremental sheet forming process of Ti6Al4 vartificial hip joint component. *Journal of Computational Science*, *60*, Article 101595. https://doi.org/10.1016/j.jocs.2022.101595

Szpunar, M., Ostrowski, R., Trzepieciński, T., & Kaščák, Ľ. (2021). Central composite design optimisation in single point incremental forming of truncated cones from commercially pure titanium Grade 2 sheet metals. *Materials*, *14*(13), Article 3634. https://doi.org/10.3390/ma14133634

Wpływ Parametrów Procesu Kształtowania Punktowego na Chropowatość Powierzchni Zewnętrznej Wytłoczek Stożkowych Wykonanych z Blach Tytanowych

Streszczenie

Wraz z upowszechnieniem obrabiarek sterowanych numerycznie, proces punktowego formowania przyrostowego cieszy się rosnącym zainteresowaniem w przemyśle. W artykule przedstawiono wyniki badań wpływu parametrów procesu formowania (krok narzędzia, prędkość obrotowa narzędzia, prędkość posuwu i strategia formowania) na chropowatość powierzchni zewnętrznej wytłoczek stożkowych kształtowanych z blach tytanowych o czystości technicznej. Przeanalizowano dwa podstawowe parametry chropowatości, średnią arytmetyczną wysokość powierzchni Sa i maksymalną wysokość powierzchni Sz. Wpływ parametrów procesu kształtowania przyrostowego na chropowatość powierzchni analizowano przy użyciu wielowarstwowych sztucznych sieci neuronowych. Stwierdzono, że zmniejszenie prędkości posuwu przy przeciwbieżnej strategii obróbki powoduje zmniejszenie średniej chropowatości Sa. Odwrotną zależność zaobserwowano podczas formowania według strategii współbieżnej. Przy małej prędkości posuwu narzędzia (500 mm/min) zmniejszenie wartości kroku narzędzia spowodowało wzrost parametru Sz. Przy dużej prędkości posuwu narzędzia (2000 mm/min) wpływ wartości kroku narzędzia jest pomijalny.

Słowa kluczowe: sztuczne sieci neuronowe, przyrostowe kształtowanie blach, kształtowanie blach, SPIF, chropowatość powierzchni